

# Journal of Biomedical Optics

[SPIDigitalLibrary.org/jbo](http://SPIDigitalLibrary.org/jbo)

## **Repeated freeze-thawing of bone tissue affects Raman bone quality measurements**

John-David P. McElderry  
Matthew R. Kole  
Michael D. Morris

# Repeated freeze-thawing of bone tissue affects Raman bone quality measurements

John-David P. McElderry, Matthew R. Kole, and Michael D. Morris

University of Michigan, Department of Chemistry, 930 N. University Avenue, Ann Arbor, Michigan 48109

**Abstract.** The ability to probe fresh tissue is a key feature to biomedical Raman spectroscopy. However, it is unclear how Raman spectra of calcified tissues are affected by freezing. In this study, six transverse sections of femoral cortical bone were subjected to multiple freeze/thaw cycles and probed using a custom Raman microscope. Significant decreases were observed in the amide I and amide III bands starting after two freeze thaw cycles. Raman band intensities arising from proline residues of frozen tissue appeared consistent with fresh tissue after four cycles. Crystallinity values of bone mineral diminished slightly with freezing and were noticeable after only one freezing. Mineral carbonate levels did not deviate significantly with freezing and thawing. The authors recommend freezing and thawing bone tissue only once to maintain accurate results. © 2011 Society of Photo-Optical Instrumentation Engineers (SPIE). [DOI: 10.1117/1.3574525]

Keywords: Raman spectroscopy; bone; freeze; thaw; apatite; tissue decomposition.

Paper 10561SSR received Oct. 15, 2010; revised manuscript received Jan. 12, 2011; accepted for publication Jan. 14, 2011; published online Jul. 1, 2011.

## 1 Introduction

The preservation of bone tissue for Raman spectroscopic analysis is essential for maintaining physical and material properties for continued or repeated experimentation. Fixing and embedding bone as a preservation technique has been studied for Fourier transform infrared spectroscopy<sup>1-4</sup> and has been widely used for Raman spectroscopy with similar success.<sup>5,6</sup> However, fixing agents can alter tissue components from their native state. Ethanol denatures bone matrix proteins and dissolves lipids. Fixing bone in ethanol perturbs protein secondary structure. Formalin binds to proteins and forms cross-links which perturb the tertiary structure of proteins but has little effect on the amide bonding.<sup>7</sup> The addition of any fixing agent comes with added complexity in the spectral background which can be challenging to remove.

Within the last 10 years, it has become apparent that probing bone using Raman spectroscopy is best completed on fresh or frozen tissues.<sup>6,8-13</sup> Raman bone studies involving other testing where the tissue cannot be fixed often require multiple steps and specimens are therefore frozen and thawed several times. This can be problematic since little is understood about the effects of freezing and thawing on Raman bands.

Mechanical tests of frozen collagenous tissues compared to fresh tissues shows that effects can be evident after freezing.<sup>14-18</sup> Compressive stress tests on knee cartilage showed comparable decreases in stiffness for both slow frozen ( $-20^{\circ}\text{C}$ ) and flash frozen ( $-80^{\circ}\text{C}$ ) tissues.<sup>14</sup> Hydration tests on frozen intervertebral disks revealed increased permeability through the collagenous layers which increased the water content in the disk nucleus.<sup>16-18</sup> However, it was noted by Bass et al. that water content was reduced within the collagen layers after freezing despite the increased permeability.<sup>17</sup>

How many times can a bone be frozen before it yields erroneous spectroscopic data? It is the aim of the authors to address this question in terms of Raman microspectroscopy. By submitting cortical bone to repeated freezing and thawing, we have identified changes in key spectral features as a result of bone degradation. It is not our aim to provide a rigorous analysis of the biology of bone degradation.

## 2 Materials and Methods

### 2.1 Preparation of Mouse Femora

Six femora were harvested fresh from 20 day old male C57BL/6 mice and all soft tissue was removed. Femora were immediately attached to a glass microscope slide with the posterior side of the mid-diaphysis facing upward using glue (Instant Crazy Glue, Elmer's Products, Inc., Columbus, Ohio). The glue was allowed to set for more than 20 min, but no more than 30 min. Femora were then polished transversely using a range of fine polishing paper (1200, 2000, 3000 grit) by inverting the slide/femur and gently gliding the bone against the paper in a figure-eight motion. Several drops of  $1\times$  Hank's balanced salt solution (HBSS) were used to lubricate the polishing surface. Femora were polished until an optically flat and smooth region was achieved in the mid-diaphysis, which was approximately 2-mm long. A notch was made with a scalpel perpendicular to the long axis at one end of the region of interest to create a landmark for reproducible orientation under a microscope.

All experiments on tissue designated as freeze thaw cycle 0 (FTC 0) were finished within 3 h of femoral extraction and within 6 h of sacrifice. Femora were individually wrapped in HBSS-soaked gauze and frozen at  $-23^{\circ}\text{C}$  for at least 12 h. Bones were then thawed at room temperature using HBSS solution for approximately 30 min before acquisition of spectra. The bones

Address all correspondence to: Michael D. Morris, University of Michigan, Department of Chemistry, 930 N University Avenue, Ann Arbor, Michigan 48109. Tel: 734 764-7360; Fax: 734 764-7360; E-mail: mdmorris@umich.edu.

were kept moist at all times during the experiment. This process was repeated four times for each bone.

## 2.2 Raman Microscopy

Specimens were loaded onto the stage of a custom-built Raman microscope comprising a fluorescence microscope (Eclipse ME600, Nikon Instruments Inc., Melville, New York), a 785-nm stabilized diode laser (Invictus, Kaiser Optical Systems, Inc., Ann Arbor, Michigan), imaging spectrograph with a 50- $\mu\text{m}$  slitwidth (Holospec f/1.8i, Kaiser Optical Systems, Inc.), and deep depletion, back-illuminated CCD camera (Classic CCD, Andor Technologies, South Windsor, Connecticut). The laser was expanded through a 20 $\times$ , 0.75 NA objective along one axis ( $100 \times 7 \mu\text{m}$ ) for line-scan imaging. Each line was averaged across the spatial axis. Twelve line spectra were acquired per specimen using 25- $\mu\text{m}$  step sizes starting with the laser line parallel to the notch. Spectral integration was 90 s per step. Post-processing of spectra was performed using calibration and baselining techniques commonly practiced in the field.

## 2.3 Bone Metrics

Several Raman spectroscopic parameters were used to assess the changes in the matrix component of cortical bone such as the normalized height of amide I ( $1664 \text{ cm}^{-1}/959 \text{ cm}^{-1}$ ), amide III ( $1270 \text{ cm}^{-1}/959 \text{ cm}^{-1}$ ), proline and hydroxyproline ( $[853 \text{ cm}^{-1} + 876 \text{ cm}^{-1}]/959 \text{ cm}^{-1}$ ), and the  $\text{CH}_2$  scissor mode ( $1450 \text{ cm}^{-1}/959 \text{ cm}^{-1}$ ). Mineral parameters such as crystallinity ( $959 \text{ cm}^{-1}$  inverse FWHM) and carbonate content ( $1070 \text{ cm}^{-1}/959 \text{ cm}^{-1}$  height ratio) were also used. Weak matrix bands at 924 and 943  $\text{cm}^{-1}$  were digitally resolved from the phosphate band using the Marquardt nonlinear curve fitting algorithm.<sup>19</sup> The carbonate band was digitally resolved using the curve fitting technique which was described by Awonusi et al.<sup>20</sup> A repeated-measures one-way analysis of variance with post-hoc analysis was performed to assess changes in each metric. Within-group significance was measured using Greenhouse–Geisser probabilities. Pairwise significance was measured only between the FTC 0 group and subsequent FTC group using Bonferonni corrected probabilities. All statistical analysis was

completed using a standard statistical software package (SSPS, IBM Corp.).

## 3 Results

After repeated freezing and thawing, the femora were visibly degraded. The notch made in the tissue for orientation purposes became less distinct and the surface became less smooth as evidenced by a reduction of focus. Small bits of soft tissue were found adhered to the gauze after later FTCs. In spite of the noticeable physical degradations, Raman spectra were consistently obtained in a reproducible location through all FTCs. It was difficult to acquire spectra beyond FTC 4 due to the loss of focus and orientation.

Repeated freezing and thawing of the femora induced significant changes in the amide bands as shown in Fig. 1. The amide I band height ( $p = 0.01$ , within FTC groups) had an overall decrease of 21%. Pairwise differences were significant after only two FTCs and trended toward significance after one FTC. The amide III band height ( $p = 0.03$ , within FTC groups) decreased 11% with significant pairwise differences after three FTCs and a trend toward significance in FTC groups 1 and 2. The pro/hyp band combination and the  $\text{CH}_2$  scissoring band did not change significantly from the unfrozen tissue.

Mineral parameters were also investigated for degradation through freezing and thawing and are shown in Fig. 2. Crystallinity values were consistent between mice as evidenced by small variances ( $\sim 1\%$  relative standard deviation) within each group. Crystallinity did change significantly ( $p = 0.003$ , within FTC groups), decreasing by 4%. Declining values of the crystallinity parameter were measured after only one FTC and more notably after three and four FTCs in pairwise comparisons with the FTC 0 group. Mineral carbonate substitution did not show a significant change after four FTCs. Positions of the phosphate and carbonate bands did not fluctuate by more than half a wavenumber.

## 4 Discussion

Degradation of the tissue was evident in Raman spectra which show changes in both mineral and matrix bands with the most pronounced changes in the amide band heights. Band area ratios

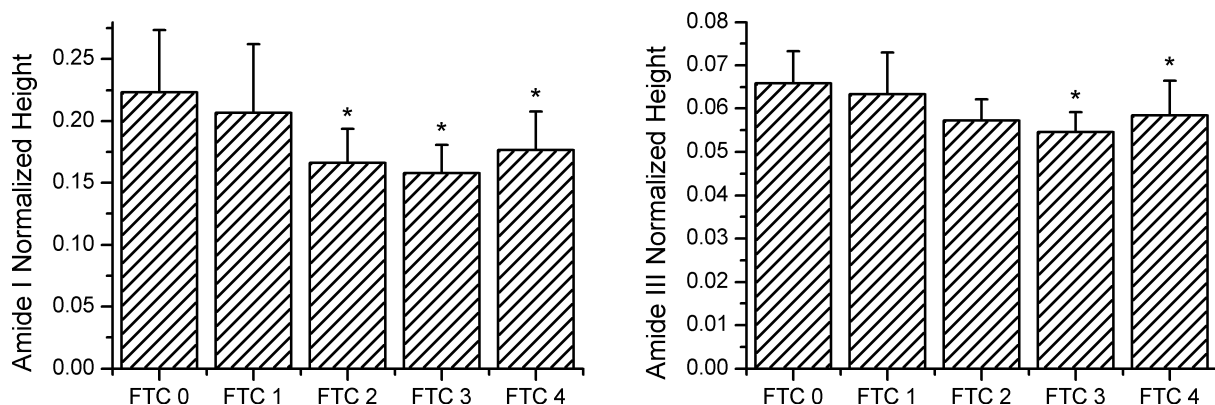


**Fig. 1** Raman measurements of the amide I and amide III band heights on cortical bone. Changes in band heights were first evident in amide I after FTC 2, and then in amide III after FTC 3. The FTC 1 group may also be indicative of subtle changes in the bone as it deteriorates. Asterisks are indicative of a Bonferonni pairwise difference from FTC 0 with significance of  $p < 0.05$ .

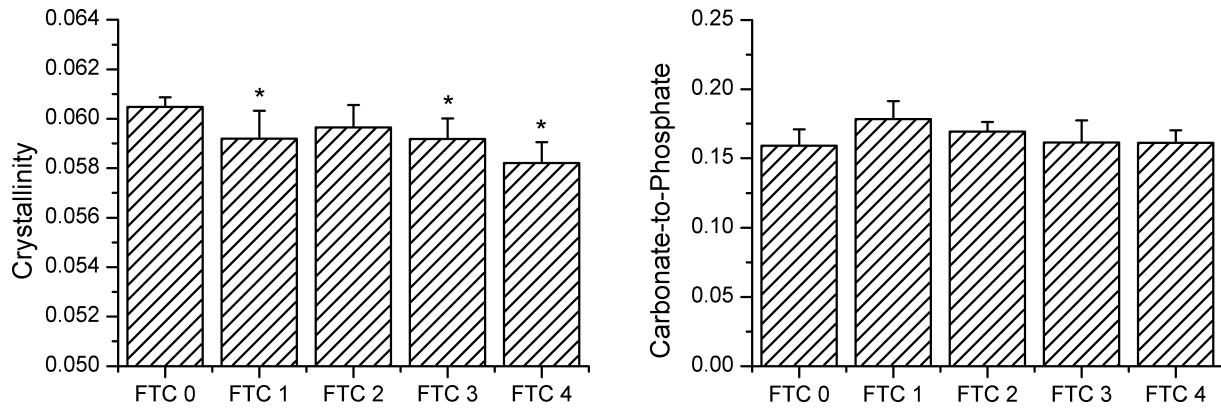


**Fig. 2** Crystallinity and carbonate-to-phosphate Raman measurements on cortical bone. Crystallinity showed decreased levels after one FTC and further decline after subsequent freezing and thawing while carbonate levels did not vary significantly. Asterisks are indicative of a Bonferonni pairwise difference from FTC 0 with significance of  $p < 0.05$ .

were also measured for the amide bands and found to be consistent with the decreases shown in Fig. 1. It is unclear whether these spectroscopic changes are indicative of actual matrix removal from the cortical bone or simply changes in the optical properties of the tissue. However, the changes in the matrix due to freezing and thawing seemed to affect the amide bands more than other matrix bands. The similarity in trend between the amide I and amide III bands suggests degradation of the protein secondary structure or denaturation. There were no pronounced changes in the pro/hyp bands that would indicate loss of collagen in the bone matrix.

Mineral measurements revealed declining crystallinity while carbonate content remained unchanged. The precision of the two measurements differed substantially. The 1020 to 1080  $\text{cm}^{-1}$  region is complicated with several phosphate peaks ( $\nu_3$ ) of comparable height which carbonate overlaps. Fitting multiple components decreases the accuracy of curve-fit estimates. A power analysis ( $\alpha = 0.95$ ,  $\beta = 0.8$ ) of the pooled standard deviations revealed that changes in carbonate levels of  $>13\%$  could be de-

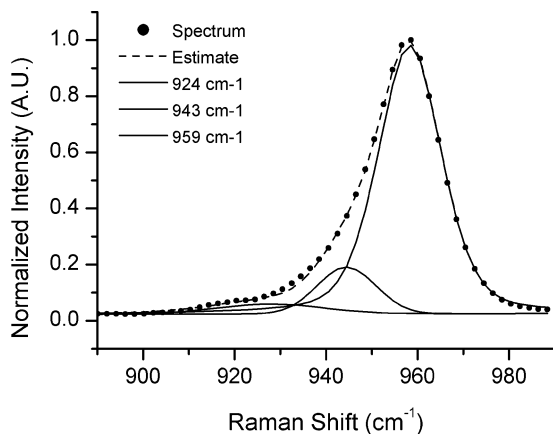


**Fig. 3** Nonlinear curve fitting results for the 882 to 982  $\text{cm}^{-1}$  region. Three Gaussian/Lorentzian functions were used to represent the phosphate 959  $\text{cm}^{-1}$  band and two matrix bands at 943 and 924  $\text{cm}^{-1}$ . Region was truncated to not include the phenylalanine band at 1002  $\text{cm}^{-1}$  and the proline and hydroxyproline bands at 853 and 876  $\text{cm}^{-1}$ . Fitting the band reveals the true symmetry of the underlying phosphate peak.

tested. By the same analysis, crystallinity was found to be much more sensitive as it was capable of detecting  $>2\%$  changes. The 900 to 990  $\text{cm}^{-1}$  region could be consistently fit to three components, shown in Fig. 3, across the region of cortical bone. This fit can be reproduced in mature wild-type mouse cortical bone. Not accounting for the matrix bands at 924 and 943  $\text{cm}^{-1}$  results in a 10% overestimation of the bandwidth. This means that changes in phosphate bandwidth could be detected down to  $<1 \text{ cm}^{-1}$  on a spectrograph with 6  $\text{cm}^{-1}$  resolution. It is clear that any changes occurring to the mineral due to freezing and thawing are small and below the detection limits of current carbonate-to-phosphate measurements.

The crystallinity parameter is an estimate of crystal size along the  $c$ -axis but can be influenced by several confounding factors. Ionic substitution by carbonate or other ions lowers crystal perfection which is reflected in lower crystallinity values. The molecular environment at the mineral surface can either induce or prevent ordering of surface ions into a stable apatitic form. Lastly, randomization of crystal orientation is capable of decreasing the apparent crystallinity. Therefore, crystallinity should be thought of as a lower limit to the crystal size. This study is incapable of distinguishing which factor is responsible for the apparent decrease in crystallinity values. However, the release of mineral from denatured matrix proteins may be sufficient to lower crystallinity values either by randomization of crystal orientation or by destabilization of surface ions.

Freezing and thawing bone multiple times results in spectral artifacts similar to fixation but to a lesser extent. Pleshko et al. measured FTIR spectra of bone fixed in ethanol and formalin showing that ethanol led to artifacts in the amide region while formalin slightly altered mineral crystallinity.<sup>2</sup> Although freezing and thawing displayed alterations in both the amide and mineral bands, they were only sizeable after several cycles. Therefore, for best results it is recommended that Raman spectroscopy studies of bone be limited to one freezing and thawing.

## 5 Conclusion

Degradation of bone tissue after repeated freezing and thawing had a significant impact on both matrix and mineral spectroscopic features and may interfere with bone quality measurements as early as one freezing.

### Acknowledgments

This study was supported in part by NIH Grant No. R01 AR047969. J.-D.M. acknowledges support through training Grant No. T90 DK070071. The authors would like to thank Guisheng Zhao for providing mice for this study.

### References

1. A. L. Boskey, M. L. Cohen, and P. G. Bullough, "Hard tissue biochemistry: A comparison of fresh-frozen and formalin-fixed tissue samples," *Calcif. Tissue Int.* **34**, 328–331 (1982).
2. N. L. Pleshko, A. L. Boskey, and R. Mendelsohn, "An FT-IR microscopic investigation of the effects of tissue preservation on bone," *Calcif. Tissue Int.* **51**, 72–77 (1991).
3. S. Aparicio, S. B. Doty, N. P. Camacho, E. P. Paschalis, L. Spevak, R. Mendelsohn, and A. L. Boskey, "Optimal methods for processing mineralized tissues for Fourier transform infrared microspectroscopy," *Calcif. Tissue Int.* **70**, 422–429 (2002).
4. N. L. Pleshko, A. L. Boskey, and R. Mendelsohn, "An infrared study of the interaction of polymethyl methacrylate with the protein and mineral components of bone," *J. Histochem. Cytochem.* **40**(9), 1413–1417 (1992).
5. Y. N. Yeni, J. Yerramshetty, O. Akkus, C. Pechey, and C. M. Les, "Effect of fixation and embedding on Raman spectroscopic analysis of bone tissue," *Calcif. Tissue Int.* **78**(6), 363–371 (2006).
6. A. Carden and M. D. Morris "Application of vibrational spectroscopy to the study of mineralized tissues," *J. Biomed. Opt.* **5**(3), 259–68 (2000).
7. A. Scarano, G. Iezzi, and A. Piattelli, "Common Fixatives In Hard-Tissue Histology," in *Handbook of Histology Methods for Bone and Cartilage*, Y. H. An and K. L. Martin, Eds., Humana Press, New Jersey (2003).
8. K. A. Dooley, J. McCormack, D. P. Fyhrie, and M. D. Morris, "Stress mapping of undamaged, strained, and failed regions of bone using Raman spectroscopy," *J. Biomed. Opt.* **14**(4), 044018 (2009).
9. M. V. Schulmerich, J. H. Cole, K. A. Dooley, M. D. Morris, J. M. Kreider, S. A. Goldstein, S. Srinivasan, and B. W. Pogue, "Noninvasive Raman tomographic imaging of canine bone tissue," *J. of Biomed. Opt.*, **13**(2), 020506 (2008).
10. M. V. Schulmerich, K. A. Dooley, M. D. Morris, T. M. Vanasse, and S. A. Goldstein, "Transcutaneous fiber optic Raman spectroscopy of bone using annular illumination and a circular array of collection fibers," *J. of Biomed. Opt.* **11**(6), 060502 (2006).
11. K. A. Dooley, J. McCormack, D. P. Fyhrie, and M. D. Morris, "Stress mapping of undamaged, strained, and failed regions of bone using Raman spectroscopy," *J. Biomed. Opt.* **14**(3), 044018 (2009).
12. J. W. Ager, R. K. Nalla, K. L. Breeden, and R. O. Ritchie, "Deep-ultraviolet Raman spectroscopy study of the effect of aging on human cortical bone," *J. Biomed. Opt.* **10**(3), 034012 (2005).
13. M. D. Morris, P. Matousek, M. Towrie, A. W. Parker, A. E. Goodship, and E. R. Draper, "Kerr-gated time-resolved Raman spectroscopy of equine cortical bone tissue," *J. Biomed. Opt.* **10**(1), 14014 (2005).
14. E. A. Kennedy, D. S. Tordonado, and S. M. Duma, "Effects of freezing on the mechanical properties of articular cartilage," *Biomed Sci. Instrum.* **43**, 342–347 (2007).
15. P. B. Lewis, J. M. Williams, N. Hallab, A. Viridi, A. Yanke, and B. J. Cole, "Multiple freeze-thaw cycled meniscal allograft tissue: A biomechanical, biochemical, and histologic analysis," *J. Orthopaed. Res.* **26**(1), 49–55 (2008).
16. M. Hongo, R. E. Gay, J. T. Hsu, K. D. Zhao, B. Ilharborde, L. J. Berglund, and K. N. An, "Effect of multiple freeze-thaw cycles on intervertebral dynamic motion characteristics in the porcine lumbar spine," *J. Biomech.* **41**, 916–920 (2008).
17. E. C. Bass, N. A. Duncan, J. S. Hariharan, J. Dusick, H. U. Bueff, and J. C. Lotz, "Frozen storage affects the compressive creep behavior of the porcine intervertebral disc," *Spine* **22**(24), 2867–2876 (1997).
18. B. Johnstone, J. P. G. Urban, S. Roberts, and J. Menage, "The fluid content of the human intervertebral disc," *Spine* **17**, 412–416 (1992).
19. W. H. Press, S. A. Teukolsky, W. T. Vetterling, and B. P. Flannery, *Numerical Recipes in C: The Art of Scientific Computing*, Cambridge University Press, Cambridge (1992).
20. A. Awonusi, M. D. Morris, and M. M. J. Tecklenburg, "Carbonate assignment and calibration in the Raman spectrum of apatite," *Calcif. Tissue Int.* **81**(1) 46–52 (2007).